

# Cosmic Ray Acceleration by Supernova Shocks

E. G. Berezhko

*Yu. G. Shafer Institute of Cosmophysical Research and Aeronomy  
31 Lenin Ave., 678980 Yakutsk, Russia*

---

## Abstract

We analyse the results of recent measurements of nonthermal emission from individual supernova remnants (SNRs) and their correspondence to the nonlinear kinetic theory of cosmic ray (CR) acceleration in SNRs. It is shown that the theory fits these data in a satisfactory way and provides the strong evidences for the efficient CR production in SNRs accompanied by significant magnetic field amplification. Magnetic field amplification leads to considerable increase of CR maximum energy so that the spectrum of CRs accelerated in SNRs is consistent with the requirements for the formation of Galactic CR spectrum up to the energy  $\sim 10^{17}$  eV.

*Key words:* Galactic cosmic rays; Supernova remnants; Shock acceleration; Nonthermal emission: radioemission, X-rays, gamma-rays

---

## 1 Introduction

The main reason why supernova remnants (SNRs) are considered as a cosmic ray (CR) source is a simple argument about the energy required to sustain the Galactic cosmic ray (GCR) population against loss by escape, nuclear interactions and ionization energy loss. The mechanical energy input to the Galaxy from each supernova (SN) is about  $10^{51}$  erg so that with a rate of about one every 30 years the total mechanical power input from supernovae is of the order  $10^{42}$  erg/s (e.g. Berezhinsky et al., 1990). Thus supernovae have enough power to drive the GCR acceleration if there exists a mechanism for channeling about 10% of the mechanical energy into relativistic particles. The high velocity ejecta produced in the supernova explosion interacts with the ambient medium to produce a system of strong shocks. The shocks in turn

---

*Email address:* berezhko@ikfia.ysn.ru (E. G. Berezhko).

can pick up a few particles from the plasma flowing into the shock fronts and accelerate them to high energies.

The only theory of particle acceleration which at present is sufficiently well developed and specific to allow quantitative model calculations is diffusive acceleration applied to the strong shocks associated with SNRs (e.g. see Drury, 1983; Blandford and Eichler, 1987; Berezhko and Krymsky, 1988; Jones and Ellison, 1991; Malkov and Drury, 2001, for review). Considerable efforts have been made during the last years to empirically confirm the theoretical expectation that the main part of GCRs indeed originates in SNRs. Theoretically progress in the solution of this problem has been due to the development of the kinetic nonlinear theory of diffusive shock acceleration (Berezhko et al., 1996; Berezhko and Völk, 1997, 2000a). The theory includes all the most relevant physical factors, essential for SNR evolution and CR acceleration, and it is able to make quantitative predictions of the expected properties of CRs produced in SNRs and their nonthermal radiation.

Detail information about high-energy CR population in SNRs can be obtained from the observations of the nonthermal emission produced by accelerated CRs in SNRs. The electron CR component is evident in a wide wave length range by the radiation that they produce in SNRs, from radio to  $\gamma$ -ray emission, whereas in the case of the nuclear CR component a  $\gamma$ -ray detection is the only possibility to find it. If this nuclear component is strongly enhanced inside SNRs then through inelastic nuclear collisions, leading to pion production and subsequent decay,  $\gamma$ -rays will be produced at the detectable level.

High-energy  $\gamma$ -rays can also be produced by CR electrons due to the inverse Compton (IC) scattering of the background photons. Therefore it is not so obvious which CR component (nuclear or electron) produces TeV emission, detected from Cassiopeia A (Cas A) (Aharonian et al., 2001), RXJ1713.7-3946 (Murashi et al., 2000; Enomoto et al., 2002; Aharonian et al., 2005, 2006a) and Vela Jr (Aharonian et al., 2006b). For this determination the SNR magnetic field value plays the crucial role. The relative role of electrons in  $\gamma$ -ray production is low if SNR magnetic field is strongly amplified. In addition, if the magnetic fields in SNRs are considerably larger than the typical interstellar value, then SNRs are able to generate a power-law spectrum of accelerated CRs at least up to the knee energy (Berezhko and Ksenofontov, 1999; Berezhko and Völk, 2004). In fact, there is strong evidence that the actual magnetic field in SNRs is indeed intrinsically enhanced: the analysis of the nonthermal emission of young SNRs show that all of them have amplified fields (Völk et al., 2005; Parizot et al., 2006). Required strength of the magnetic field, that is significantly higher than the interstellar medium (ISM) field, has to be attributed to nonlinear field amplification at the SN shock by CR acceleration itself, in fact by the dominant nuclear CR component (Lucek and Bell, 2000; Bell, 2004).

The application of kinetic theory to individual SNRs (see Berezhko, 2005, for a review) has demonstrated its power in explaining the observed SNR properties and in predicting new effects like the extent of magnetic field amplification, leading to the concentration of the highest-energy electrons in a very thin shell just behind the shock. The theory also predicted the enhancement of the high-energy galactic  $\gamma$ -ray background radiation due to the contribution of CRs confined in parent SNRs, that was partly confirmed by the measured background TeV-emission.

In order to perform the detail comparison of theoretical expectation with the experiment one needs sufficient number of individual SNRs with known values of relevant physical parameters such as the age, distance, ISM density. Unfortunately the number of such SNRs are very limited, especially those which are seen in all wavelength from radio to  $\gamma$ -ray. It is why every new experimentally established property of nonthermal emission of SNR represents considerable interest for theoretical analysis. Therefore we start this review with a brief consideration of three SNRs for which essentially new information about the efficiency of CR production was recently obtained. Then we shall consider the correspondence of the interior magnetic field values extracted from the analysis of the experimental data with theoretical expectation. Finally, we discuss the maximum energy of CRs which can be achieved during their acceleration in SNRs, taking into account realistic values of magnetic field in SNRs.

## 2 Evidences for efficient CR production in SNRs

Experimental and theoretical study of young galactic SNRs, Tycho's SNR, RX J1713.7-3946 and SN 1987A, performed recently provides very useful information about CR acceleration by SN shocks. Therefore below we briefly analyse these results.

### 2.1 Tycho's supernova remnant

The kinetic theory has been applied in detail to Tycho's SNR, the result of a type Ia SN explosion in a (roughly) uniform interstellar medium (ISM), in order to compare the results with existing data, using a stellar ejecta mass  $M_{ej} = 1.4M_{\odot}$ , distance  $d = 2.3$  kpc, and ISM number density  $N_H = 0.5$  H-atoms  $\text{cm}^{-3}$  (Völk et al., 2002, 2005). For these parameters a total hydrodynamic explosion energy  $E_{sn} = 0.27 \times 10^{51}$  erg was derived to fit the observed size  $R_s$  and expansion speed  $V_s$ . A rather high downstream magnetic field strength  $B_d \approx 300 \mu\text{G}$  is needed to reproduce the observed steep and concave radio spectrum (see also Reynolds and Ellison, 1992) and to ensure a

smooth cutoff of the synchrotron emission in the X-ray region. Overall, very good consistency of the predictions of the nonlinear theory with the existing observational data was achieved.

Using Chandra X-ray observations Warren et al. (2005) have recently estimated the ratio between the radius  $R_c$  of the contact discontinuity (CD), separating the swept-up ISM and the ejecta material, and the radius  $R_s$  of the forward shock. The large mean value  $R_c/R_s = 0.93$  of this ratio was interpreted as evidence for efficient CR acceleration, which makes the medium between those two discontinuities more compressible. This result was analysed within already performed kinetic nonlinear approach (Völk et al., 2006). Note, that the increase of the ratio  $R_c/R_s$  due to the SN shock modification by efficiently accelerated CRs was predicted for the case of Kepler’s SNR by Decourchelle et al. (2000).

Fig.1 and Fig.2 show the calculations of shock and CD related quantities which were part of the earlier considerations (Völk et al., 2002, 2005), together with the azimuthally averaged experimental data available at the time. The calculated shock as well as CD radii and speeds are shown as a function of time for the two different cases of interior magnetic field strengths  $B_d = 240 \mu\text{G}$  and  $B_d = 360 \mu\text{G}$  required by the value of the synchrotron frequency, where the spectrum hardens relative to the low-energy radio spectrum.

According to Fig.1a Tycho’s SNR is nearing the adiabatic phase. The softness of the observed low-energy radio spectrum – relative to a test particle spectrum – required a proton injection rate  $\eta = 3 \times 10^{-4}$ . This implies a significant nonlinear modification of the shock at the current age of  $t = 428$  yrs. A larger magnetic field lowers the Alfvénic Mach number and therefore leads to a decrease of the shock compression ratio, as seen in Fig.1b. The result is a total compression ratio  $\sigma = 5.7$  and a subshock compression ratio  $\sigma_s = 3.5$  for  $B_d = 240 \mu\text{G}$ . In turn  $\sigma = 5.2$ ,  $\sigma_s = 3.6$ , for  $B_d = 360 \mu\text{G}$ .

Therefore, including CR acceleration at the outer blast wave, the calculated value of the ratio  $R_c/R_s$  for  $B_d = 360 \mu\text{G}$  is slightly lower than for  $B_d = 240 \mu\text{G}$ . At the current epoch we have  $R_c/R_s \approx 0.90$  which is somewhat lower than the value  $R_c/R_s = 0.93$  inferred from the Chandra observations.

Projecting a highly structured shell onto the plane of the sky tends to favor protruding parts of the shell. Therefore the average radius measured in projection is an overestimate of the true average radius. Analyzing the amount of bias from the projection for the shock and CD radii Warren et al. (2005) found a corrected ”true” value  $R_c/R_s = 0.93$  which is lower than their measured “projected average” value  $R_c/R_s = 0.96$ . One needs to make such a purely geometrical correction independently of the nature of the factors which produce the shell structures, if one measures the size of the quasispherical

structured shell in projection instead of dealing with a 2-dimensional shell cross-section. In the latter case there would be no need for such a correction.

Irrespective of this need to correct the observations of the CD position, if one starts from a spherically symmetric calculation of the CD radius as we do, one has to take into account that the actual CD is subject to the Rayleigh-Taylor (R-T) instability (e.g. Chevalier et al., 1992; Wang and Chevalier, 2001), and thus a correction is needed to compare such a 1-D calculation with observations of the CD. In the nonlinear regime the instability leads to effective mixing of the ejecta and swept-up ISM material with “fingers” of the ejecta on top of this mixing region. The latter has a radius larger than  $R_c^{1D}$ . The minimum correction to  $R_c^{1D}$  is the radial extent  $\Delta R_c$  of the mixing region above  $R_c^{1D}$ . We estimate  $\Delta R_c \approx 0.5l$ , where  $l \approx 0.1R_c^{1D}$  is the longest finger size according to the numerical modeling of Wang and Chevalier (2001) (albeit without particle acceleration). This leads to a rough estimate of the corrected CD radius  $R'_c = 1.05R_c^{1D}$ .

As it is seen in Fig.2, the comparison of the corrected values  $R'_c/R_s$ , according to the earlier calculations (Völk et al., 2002, 2005), with this experimentally estimated value  $R_c/R_s = 0.93$  shows quite good agreement.

The agreement between theoretical solutions for effective particle acceleration with the measurements of the shock and discontinuity radii has to be considered as new evidence for strong nonthermal effects in Tycho’s SNR. New Northern Hemisphere TeV detectors is expected to detect this source at TeV-energies in, predominantly, hadronic  $\gamma$ -rays at an energy flux level above  $2 \times 10^{-13} \text{erg cm}^{-2} \text{s}^{-1}$ . As a corollary the detection of a TeV signal is not only important by itself, but it is also crucial for the correct determination of all other key SNR parameters.

## 2.2 *Supernova remnant RX J1713-3946*

RX J1713-3946 is a shell-type supernova remnant (SNR), located in the Galactic plane, that was discovered in X-rays with ROSAT (Pfeffermann and Aschenbach, 1996). Further study of this SNR with the ASCA satellite by Koyama et al. (1997) and later by Slane et al. (1999) have shown that the observable X-ray emission is entirely non-thermal, and this property was confirmed in later XMM-Newton observations (Cassam-Chenaï et al., 2004). The radio emission of this SNR is weak: only part of the shell could be detected in radio synchrotron emission up to now, with a poorly known spectral form (Lazendic et al., 2004).

RX J1713-3946 was also detected in very high energy  $\gamma$ -rays with the CANGAROO (Murashi et al., 2000; Enomoto et al., 2002) and H.E.S.S. (Aharonian et al.,

2006a) telescopes. Especially the latter observations show a clear shell structure at TeV energies which correlates well with the ASCA contours.

The difficulty for the theoretical description is the fact that several key parameters of this source are either not known or poorly constrained. This already concerns the distance and age of the object. It was demonstrated that consistent description of this object is achieved (Berezhko and Völk, 2006) following present consensus which puts the distance at 1 kpc, the age to about 1600 years and that the primary explosion must have been a type II/Ib SN event with a massive progenitor star whose mass loss in the main sequence phase created a hot wind bubble in a high-density environment. The solution for the overall remnant dynamics then yields the value for the expansion velocity of the outer shock, given the total mechanical energy  $E_{\text{sn}} = 1.8 \times 10^{51}$  erg released in the explosion. To obtain a consistent solution for the broadband nonthermal emission the injection rate  $\eta = 3 \times 10^{-4}$  and interior magnetic field  $B_d \approx 130 \mu\text{G}$  are needed.

The calculated overall broadband spectral energy distribution is displayed in Fig.3, together with the experimental data from ATCA at radio wavelengths, as estimated for the full remnant by Aharonian et al. (2006a), the X-ray data from ASCA, and the most recently measured TeV gamma-ray spectrum from H.E.S.S. (Aharonian et al., 2007). The overall fit is impressive, noting that the choice of a few key parameters like  $\eta$ ,  $B_d$ ,  $E_{\text{sn}}$  in the theory allows a spectrum determination over more than 19 decades. Note, that calculated gamma-ray spectrum (Berezhko and Völk, 2006) agrees with the new H.E.S.S. data (Aharonian et al., 2007) even better than with earlier H.E.S.S. measurements (Aharonian et al., 2006a).

The properties of small scale structures of SNR RX J1713.7-3946 seen in X-rays by Uchiyama et al. (2003), and in particular by Hiraga et al. (2005), provide even stronger evidence that the magnetic field inside the SNR is indeed considerably amplified.

In order to find out if the filamentary structure found by (Hiraga et al., 2005) is indeed consistent with the efficient CR production projected radial profile  $J(\epsilon_\nu, \rho)$  calculated for the X-ray energy  $\epsilon_\nu = 1$  keV is shown in Fig.4. The theory predicts the peak of the emission just behind the shock front with projected thickness  $\Delta\rho/R_s \approx 10^{-2}$  that corresponds to an angular width  $\Delta\psi \approx 0.4'$ . This width is significantly thinner than the observed width of  $\Delta\psi \approx 2.2'$ . However, one should take into account the smoothing procedure with which the data were obtained/presented. If we apply a point spread function of width  $\sigma_\psi = 12.8''$ , corresponding to the smoothed XMM data, to the calculated profile, we obtain the broadened profile, which is shown in Fig.4 by the dashed curve. It has a width  $\Delta\rho/R_s \approx 6.6 \times 10^{-2}$ , or  $\Delta\psi \approx 2'$ , and is consistent with the observational profile of Hiraga et al. (2005).

In addition the projected radial profile (dash-dotted line) which corresponds to the test particle limit is presented in Fig.4. In this case the proton injection rate was taken artificially so small ( $\eta = 10^{-5}$ ), that accelerated CRs do not produce any significant nonlinear effect, like shock modification and/or magnetic field amplification. Therefore interior magnetic field value  $B_d = 20 \mu\text{G}$  is much lower in this case. Due to this fact synchrotron losses are not relevant on account of the low magnetic field, the peak of the emission is broader by a factor of five, inconsistent with the XMM observations.

The projected radial  $\gamma$ -ray emission profile, calculated for the energy  $\epsilon_\gamma = 1 \text{ TeV}$ , is presented in Fig.5. As a result of the large radial gradient of the gas density and the CR distribution inside the SNR, the theoretically predicted radial profile of the TeV-emission is concentrated within a thin shell of width  $\Delta\rho \approx 0.1R_s$ . Since the H.E.S.S. instrument has a finite angular resolution we present in Fig.4 also the modified radial profile smoothed with the Gaussian point spread function with  $\sigma_\rho = \Delta\rho = 0.08R_s$ , that corresponds to the angular resolution  $2\sigma_\psi = 0.1^\circ$ .

As shown by Fig.5 the smoothed radial profile of the TeV-emission is much broader and – what is most interesting – it is characterised by a maximum to minimum intensity ratio  $J_\gamma^{\text{max}}/J_\gamma^{\text{min}} = 2.2$ . Such a ratio is consistent with the H.E.S.S. measurement (Aharonian et al., 2006a) which obviously gives only a lower limit to the sharpness of the  $\gamma$ -ray profile. Note that the broad radial profile of the TeV-emission with  $J_\gamma^{\text{max}}/J_\gamma^{\text{min}} \approx 2$  measured by the H.E.S.S. instrument is indirect evidence that the actual radial profile is significantly sharper, with a higher ratio  $J_\gamma^{\text{max}}/J_\gamma^{\text{min}} > 2.2$ .

We conclude that the present observational knowledge of SNR RX J1713.7-3946 can be interpreted by a source which ultimately converts about 10% of the mechanical explosion energy into nuclear CRs and that the observed high energy  $\gamma$ -ray emission of SNR RX J1713.7-3946 is of hadronic origin. Note, that Malkov et al. (2005) have obtained the same type of conclusion suggesting a rather different  $\gamma$ -ray spectrum formation scenario, compared with Berezhko and Völk (2006).

### 2.3 *Supernova remnant SN 1987A*

Supernova 1987A occurred in the Large Magellanic Cloud. It has been extensively studied in all wavelengths from radio to  $\gamma$ -ray . The initial short outburst of radio emission (Turtle et al., 1987) is attributed to the synchrotron emission of electrons accelerated by the SN shock propagated in the free wind of presupernova star, which was the blue supergiant (BSG) (Chevalier and Fransson, 1987). After about 3 years radio emission was detected again (Staveley-Smith et al.,

1992; Gaensler et al., 1997) as well as the monotonically increased X-ray emission (Gorenstein et al., 1994; Hasinger et al., 1996). This second increase of emission is attributed to the entrance of the outer SN shock into the thermalized BSG wind and then in the H II region occupied by much more dense matter, consists of the swept up wind of red supergiant (RSG) progenitor star (Chevalier and Dwarkadas, 1995).

The advantage of SN 1987A for theoretical consideration is that the key parameter values are very well determined: stellar ejecta mass  $M_{ej} = 10M_{\odot}$ , distance  $d = 50$  kpc, hydrodynamic explosion energy  $E_{sn} = 1.5 \times 10^{51}$  erg (e.g. McCray, 1993). During an initial period the shell material has a broad distribution in velocity  $v$ . The fastest part of this ejecta distribution is described by a power law  $dM_{ej}/dv \propto v^{2-k}$  with  $k = 8.6$ .

The kinetic nonlinear model for CR acceleration in SNRs has been in detail applied to SN 1987A, in order to compare its results with observational properties (Berezhko and Ksenofontov, 2006).

A rather high downstream magnetic field strength  $B_d > 1$  mG is needed to reproduce the observed steep radio spectrum (Berezhko and Ksenofontov, 2000). The required strength of the magnetic field have to be attributed to nonlinear field amplification at the SN shock by CR acceleration itself. Since for all the thoroughly studied young SNRs, the ratio of magnetic field energy density  $B_0^2/8\pi$  in the upstream region of the shock precursor to the CR pressure  $P_c$  is about  $B_0^2/(8\pi P_c) \approx 5 \times 10^{-3}$  (Völk et al., 2005) and CR pressure in young SNRs has a typical value  $P_c \approx 0.5\rho_0 V_s^2$ , the upstream magnetic field  $B_0 = B_d/\sigma$  was taken in the form

$$B_0 = \sqrt{2\pi \times 10^{-3} \rho_0 V_s^2}. \quad (1)$$

Calculated shock radius  $R_s$  and speed  $V_s$  shown in Fig.6a as a function of time are in satisfactory agreement with the values obtained on the basis of radio and X-ray measurements. Note that radio data compared with X-ray data gives larger shock size at any given time  $t$  and calculated radius  $R_s(t)$  goes between these two sets of data.

To fit the spectral shape of the observed radio emission a proton injection rate  $\eta = 3 \times 10^{-3}$  is needed. This leads to a significant nonlinear modification of the shock: as it is seen in Fig.6b total shock compression ratio  $\sigma \approx 5.3$  is essentially larger and a subshock compression ratio  $\sigma_s \approx 2.8$  is lower than classical value 4.

Since during the last 15 yrs the shock speed and the gas density are almost constant CR energy content grows roughly linearly with time (see Fig.6c). It gives the natural explanation of the linear increase of the radio emission



detected during this evolutionary period.

Strongly modified SN shock generates CR spectrum  $N \propto p^{-\gamma}$ , which is very steep at momenta  $p < m_p c$ , with index  $\gamma = (\sigma_s + 2)/(\sigma_s - 1) \approx 2.7$ . CR electrons with such a spectrum produces synchrotron radioemission spectrum  $S_\nu \propto \nu^{-\alpha}$  with spectral index  $\alpha = (\gamma - 1)/2 \approx 0.9$ , that very well corresponds to the experiment, as it is seen in Fig.7, where synchrotron energy spectra  $\nu S_\nu$ , calculated for five subsequent epoch together with the experimental data are presented. Note that CR spectrum has a concave shape: it becomes flatter at higher momenta  $p$ . As a consequence synchrotron spectrum  $S_\nu(\nu)$  is also concave as it is clearly seen in Fig.7 at  $\nu < 10^{12}$  Hz. Radio data reveal this property in good consistency with theoretical prediction.

Strong downstream magnetic field  $B_d \approx 15$  mG, that corresponds to the upstream field  $B_0 \approx 3$  mG (see Fig.7), provides synchrotron cooling of electrons with momenta  $p > 10m_p c$  that in turn makes synchrotron spectrum at high frequencies  $\nu > 10^{12}$  Hz very steep (see Fig.7). Concave shape of electrons continuously produced at the shock front together with their synchrotron cooling lead to a formation of two peaks in synchrotron energy spectrum  $\nu S_\nu$ . The first one at  $\nu \approx 10^{12}$  Hz corresponds to CR electron momentum  $p \approx 10m_p c$  above which synchrotron energy losses are relevant, whereas the second peak at  $\nu \approx 10^{18}$  Hz corresponds to the maximum momentum  $p \approx 10^4 m_p c$  of accelerated electrons. Under this condition calculated synchrotron flux at frequency  $\nu \approx 10^{17}$  Hz, which corresponds to the photon energy  $\epsilon_\gamma = 0.5$  keV, is below the measured flux at the epochs  $t > 3000$  d. Since the contribution of the nonthermal radiation in the observed X-ray emission of SN 1987A is not very well known (e.g. Michael et al., 2002), the observed X-ray flux has to be considered as the upper limit for the expected nonthermal emission. At early epoch  $t < 2500$  d however the calculated flux exceeds the measured one (see the curve, corresponding  $t = 1970$  d in Fig.7). This can be considered as indication, that the actual magnetic field  $B_0$  is few times larger then given by the Eq.(1).

At lower magnetic field  $B_d \approx 2$  mG synchrotron losses of high energy CR electrons are considerably smaller compared with the previous case. Due to this fact synchrotron spectra considerably exceeds at any given epoch the measured Chandra flux (Berezhko and Ksenofontov, 2006). Therefore one can conclude, that the actual interior magnetic field strength is not lower than 5 mG.

We see that quite a reasonable consistency of kinetic nonlinear theory with most of the observational data of SN 1987A is achieved, that gives the evidence of the efficient CR production leading to a strong shock modification and strong magnetic field amplification.

Calculated  $\gamma$ -ray integral energy flux at all energies is dominated by the  $\pi^0$ -decay component (Berezhko and Ksenofontov, 2006). At the current epoch the expected  $\gamma$ -ray energy flux at TeV-energies is about  $\epsilon_\gamma F_\gamma \approx 2 \times 10^{-13}$  erg/(cm<sup>2</sup>s) and during the next four years it is expected to grow by a factor of two. The detection of high energy  $\gamma$ -rays from SN 1987A, which could be done by instruments like H.E.S.S., would provide very clear evidence for the efficient acceleration of nuclear CRs.

## 2.4 Discussion

Detailed consideration performed within a frame of nonlinear kinetic theory demonstrates that the CR production efficiency in young SNRs is consistent with requirements for the Galactic CR sources. Recent experimental and theoretical studies of Tycho's SNR, RX J1713.7-3946 and SN 1987A provides new very strong evidence for that.

Consideration performed by Hillas (2005) led him to the opposite conclusion: that TeV  $\gamma$ -ray emission from the mostly fairly young SNRs (SN 1006, Cas A and Tycho's) is unexpectedly low. Note, however, that this consideration is based on the simplified estimates, which does not take into account such an important aspect as the necessity of renormalization of CR production efficiency, predicted in spherical approach. We have argued before that ion injection is quite efficient at the quasiparallel portions of the shock surface and it is expected to be strongly suppressed at the quasiperpendicular part of the shock (see Völk et al., 2003, for details). Therefore one should renormalize the results for the nucleonic spectrum, calculated within the spherically symmetric model. The lack of symmetry in the actual SNR can be approximately taken into account by a renormalization factor  $f_{re} < 1$ , roughly  $f_{re} = 0.15$  to  $0.25$ , which diminishes the nucleonic CR production efficiency, calculated in the spherical model, and all effects associated with it.

For SN 1006 which appears to approximate this ideal case, efficient CR production is expected to arise within two polar regions, where the SN shock is quasi-parallel. The calculated size of the efficient CR production regions which amounts to about 20% of the shock surface corresponds very well to the observed sizes of the bright X-ray synchrotron emission regions (Völk et al., 2003). This implies a renormalization factor of 0.2. In addition, the distance to the object  $d = 1.1$  kpc used by Hillas (2005) for the case of SN 1006 is considerably lower than the most reliable determination of the distance  $d = 2.2$  kpc to SN 1006 (Winkler et al., 2003).

Due to the above two factors the estimate of TeV  $\gamma$ -ray flux from SN 1006, made by Hillas (2005), should be reduced by a factor of 20, so that it will

be in agreement with H.E.S.S. upper limit. Note, that the study of SN 1006 on the basis of kinetic nonlinear theory demonstrated that the lack of a TeV signal that follows from the non-detection by the H.E.S.S. instrument does not invalidate the theoretical picture which gives a consistent description of the nonthermal emission characteristics; it rather implies a constraint on the ambient gas density  $N_{\text{H}} < 0.1 \text{ cm}^{-3}$  (Ksenofontov et al., 2005). Using XMM-Newton X-ray observations Acero and Ballet (2006) recently confirmed that the ISM density is indeed low,  $N_{\text{H}} < 0.1 \text{ cm}^{-3}$ . The example of SN 1006 illustrates that real difficulty in reliable prediction of expected  $\gamma$ -ray emission from SNRs is not a theoretical one, but rather due to poorly known values of relevant astronomical parameters, like distance to the object and ambient ISM density. From theoretical consideration (Ksenofontov et al., 2005) it becomes clear that in the case of SN 1006 and in other similar cases  $\gamma$ -ray measurements will at the same time give a reliable estimate of the ambient ISM density.

Similar situation is for the two other cases of Cas A and Tycho's SNR, considered by Hillas (2005): renormalization of his estimates, made in spherical approach, and the adoption the most reliable astronomical parameters provide the value of the expected  $\gamma$ -ray flux consistent with the existing measurements (or upper limits) (see Berezhko, 2005).

### 3 Amplified magnetic field in SNRs

All young SNRs (including three above cases) to which nonlinear kinetic acceleration theory has been successfully applied up to now exhibit the strongly amplified magnetic field as result of very efficient acceleration of nuclear CRs (Völk et al., 2005; Berezhko, 2005). Magnetic field extracted from the spectral properties of the overall synchrotron emission and from the observed filamentary structure of the nonthermal X-ray emission agree very well and their value can be expressed in the form

$$B_0^2/(8\pi) = 5 \times 10^{-3} P_c, \quad (2)$$

where  $P_c$  is CR pressure at the shock front,  $B_0 \gg B_{ISM}$  is the upstream field, which is already amplified and therefore considerably exceeds magnetic field value  $B_{ISM} \approx 5 \mu\text{G}$  in the ambient ISM. Let us consider the consistency of such a field strength with the plasma physics.

Several attempts have been undertaken to model highly nonlinear turbulent magnetic field, created by accelerated CRs upstream of the strong shock (Bell and Lucek, 2001; Vladimirov et al., 2006; Amato and Blasi, 2006). Two aspects of this process are of significant importance: the amount of magnetic

field amplification and the extent of of gas heating due to the turbulence dissipation. Unfortunately up to now it is not clear in which proportions CR working on the gas in the precursor region is divided between gas heating and magnetic field amplification. Therefore we restrict ourselves here by a simple estimates in order to demonstrate that considerable magnetic field amplification  $B_0 \gg B_{ISM}$ , consistent with Eq.(2) is indeed possible upstream of the strong shock.

There are two different mechanisms operating upstream of the fast super-Alfvénic shock and leading to the amplification of the chaotic magnetic field. The first one is related with the resonant interaction of CRs with the Alfvén waves, which due to the CR anisotropy triggers an instability, followed by the intense Alfvén wave excitation (Bell, 1978; McKenzie and Völk, 1982). The other one, recently proposed by Bell (2004), is non-resonant amplification of MHD perturbations due to Lorentz force, created by CR current.

Integral effect of resonant Alfvén wave excitation can be written in the form (McKenzie and Völk, 1982)

$$2u \frac{dE_B}{dx} = c_A \frac{dP_c}{dx}, \quad (3)$$

if we suggest that the CR working  $c_A dP_c/dx$  goes on the excitation of the Alfvén waves. Here  $E_B = (\delta B)^2/(8\pi)$  is magnetic component of the Alfvén wave energy density,  $c_A = B/\sqrt{4\pi\rho}$  is Alfvénic speed,  $u$  is the plasma flow speed directed along the  $x$  axis to the shock situated at the point  $x = 0$ . For the purpose of estimates we suggest quasistationary condition and neglect the gas speed variation  $u(x)$  in the upstream region  $x < 0$  due to the shock modification by CR backreaction, taking  $u = V_s$ . Assuming that the far upstream field  $B_0 = B_{ISM}$  coincides with the ISM field  $B_{ISM}$  and performing the integration of the above equation we have magnetic field energy density at the shock front

$$E_B/E_{B0} = M_{A0} P_c/(\rho u^2), \quad (4)$$

where  $M_{A0} = V_s/c_{A0}$  is Alfvénic shock Mach number,  $E_{B0} = B_0^2/(8\pi)$  is the energy density of the far upstream field. Since the strong shock provides efficient CR acceleration with  $P_c/(\rho u^2) \sim 1$  the above expression shows that Alfvén wave amplitude grows to a large value  $\delta B \gg B_0$  in the case of strong shock with Mach number  $M_{A0} \gg 1$ .

Resonant magnetic field amplification should be supplemented by two effects: non-resonant instability and the Alfvén speed variation  $c_A(B)$  across the precursor due to the increase of the mean effective field  $B$ . In this case (see

Pelletier et al., 2006, for details) instead of (4) we have

$$E_B/E_{B0} = M_{A0}(B_{nr}/B_0)P_c/(\rho u^2), \quad (5)$$

where

$$B_{nr} = B_0 \sqrt{\frac{3u^5}{\Phi c_{A0}^4 c} \frac{P_c}{\rho u^2}} \quad (6)$$

is the mean field amplified non-resonantly. Here  $\Phi = \log(p_{max}/m_p c)$ ,  $p_{max}$  is the maximum CR momentum.

Substituting  $\Phi = 10$  in the expression (5) we have

$$E_B = 3 \times 10^{-2} (V_s/3000 \text{ km/s})^{1/2} P_c. \quad (7)$$

Since for all known young galactic SNRs the shock speed is about  $V_s \approx 10^{-2}c$ , this expression shows, that existing mechanisms is able to amplify magnetic field within the precursor to the level, which considerably exceeds the required value (2). Therefore we can suggest that the main amount of the energy given by the expression (5) in fact goes on the gas heating due to dissipation of MHD perturbations and only small fraction of it, given by (2), indeed goes on the magnetic field amplification. Numerical simulation of considered process performed by Bell (2004) confirmed, that the gas thermal energy an order of magnitude larger than the energy content of amplified magnetic field.

Note that the process of magnetic field amplification is not included in kinetic nonlinear theory (e.g. Berezhko et al., 1996; Berezhko, 2005). It simply postulates the existence of already amplified far upstream field  $B_0$ , which value is consistent with experimental requirements, given by Eq.(2). The consistency of such a picture is provided by the fact, that the spectrum of CRs produced by strong modified shock is very hard so that CRs with highest energies have a largest contribution in their energy content. These the most energetic CRs produce field amplification on their spacial scale that is the precursor size. Therefore CRs with lower energies already 'see' the amplified field  $B_0 \gg B_{ISM}$ . Note also, that kinetic nonlinear model contains in the explicit form the suggestion, that the whole CR working goes on the gas heating presumably due to some kind of dissipation mechanism. Since according to the above estimates, the magnetic field energy which can be potentially achieved in the precursor region is considerably larger than required energy, given by Eq.(2), it can be considered as indirect evidence for the existence of such dissipation processes, which efficiently converts the energy of magnetic field perturbations into the gas thermal energy.

The existence of nonadiabatic gas heating within the precursor plays an important role for the shock structure and dynamics. It restricts the shock compression ratio by the value (Berezhko et al., 1996; Berezhko and Ellison, 1999)

$$\sigma \approx 1.5M_{A0}^{3/8}, \quad (8)$$

if the whole CR working  $c_A dP_c/dx$  goes on the gas heating. For the appropriate upstream magnetic field values, consistent with Eq.(2), it provides moderate shock modification with  $\sigma \approx 6$ . In the opposite case, when within the precursor there are no any additional gas heating except adiabatic one, the expected shock compression ratio is (Berezhko et al., 1996; Berezhko and Ellison, 1999)

$$\sigma \approx 1.3M_{S0}^{3/4}, \quad (9)$$

where  $M_{S0} = V_s/c_{S0}$  is the sonic Mach number,  $c_{S0}$  is the far upstream sound speed. For the typical ISM parameters this expression leads to much larger shock compression  $\sigma \gg 6$ .

In the case when CR working in the upstream region goes on the gas heating, the expected gas thermal energy just ahead of the subshock is

$$E_g \approx P_c/M_{A0}. \quad (10)$$

Appropriate magnetic field value  $B_0$  given by Eq.(2) leads to a typical shock compression ratio  $\sigma = 6$ , that according to Eq.(8) corresponds to  $M_{A0} \approx 40$ , that in turn according to Eq.(10) provides gas thermal energy  $E_g \approx 2.5 \times 10^{-2}P_c$ . This value  $E_g$  very well corresponds to what is expected from the expression (7), if indeed main amount of magnetic field perturbation energy is dissipated. We therefore conclude that kinetic nonlinear theory provides the consistent description at least at shock speeds  $V_s \sim 3000$  km/s, that correspond to the most active phase of the SNR evolution that is the beginning of the Sedov phase.

#### 4 Maximum energy of CRs

The most important consequence of magnetic field amplification in SNRs is the substantial increase of the maximum energy of CRs  $\epsilon_{max} = p_{max}c$ , accelerated by SN shocks. Let us briefly analyse what value of  $\epsilon_{max}$  can be expected taking into account the amplification of SNRs magnetic field.

According to theoretical consideration (Lucek and Bell, 2000) and the analysis of the observational data (Parizot et al., 2006) CR diffusion in the amplified

magnetic field is close to the Bohm limit. Therefore cutoff momentum of CRs accelerated at any given SNR evolutionary stage can be expressed in the form (Berezhko, 1996)

$$p_m = m_p c R_s V_s / [A \kappa(m_p c)], \quad (11)$$

where  $\kappa(p) = pc^2/(3ZeB_0)$  is CR diffusion coefficient, corresponding to Bohm limit;  $Z$  is the charge number of CR nuclei. The value of parameter  $A$  depends on the shock expansion law  $R_s(t)$  and on the downstream gas flow radial profile  $w(r)$ . Note that the main factors which determines the value of CR cutoff momentum  $p_m$  are: i) finite shock size; ii) shock deceleration and iii) CR adiabatic cooling in the expended downstream region  $r < R_s$ . These factors are more relevant compared with the time factor, studied by Lagage and Cesarsky (1983), that in turn prevents the complete shock modification due to CR backreaction (Drury et al., 1995).

First consider the most simple case of uniform ISM, that is typical for type Ia SNe. In such a case the main part of CR spectrum formed during the SNR evolution is produced at the Sedov phase. Since the CR cutoff momentum at the Sedov phase  $p_m \propto R_s V_s B_0 \propto R_s V_s^2 \propto t^{-4/5}$  decreases with time  $t$  the most energetic CRs in the power law part of this spectrum are produced at the very end of the free expansion phase. Therefore the maximum CR momentum  $p_{max} = \max\{p_m(t)\}$  depends on physical parameters as  $p_{max} \propto V_0 R_0 B_0(t_0)$ , where  $V_0$ ,  $R_0$  and  $t_0$  are mean ejecta speed, sweep up radius and sweep up time respectively. Taking into account the value of upstream magnetic field (2) and assuming  $P_c = 0.5\rho_0 V_s^2$ , we have (Berezhko and Völk, 2004)

$$\frac{p_{max}}{m_p c} = 3 \times 10^6 Z \left( \frac{E_{sn}}{10^{51} \text{ erg}} \right) \left( \frac{M_{ej}}{1.4 M_\odot} \right)^{-2/3} \left( \frac{N_H}{0.3 \text{ cm}^{-3}} \right)^{1/6}. \quad (12)$$

It has a strong dependence on the SN parameters  $E_{sn}$  and  $M_{ej}$ , but is only weakly dependent upon the ISM density  $\rho_0 = 1.4 N_H m_p$ .

Maximum momentum of protons, given by Eq.(12) for  $E_{sn} = 10^{51}$  erg,  $M_{ej} = 1.4 M_\odot$  and  $N_H = 0.3 \text{ cm}^{-3}$  is  $p_{max} \approx 3 \times 10^6 m_p c$ . This required condition to reproduce the spectrum of GCRs up to the knee energy is fulfilled due to the magnetic field amplification.

For CR iron nuclei  $p_{max} \approx 10^8 m_p c$  that provides the possibility for the formation of GCR spectrum up to the energy  $\sim 10^{17}$  eV inside SNRs.

Since during the early free expansion SNR evolutionary phase the SN shock speed  $V_s = (3 - 4) \times 10^4$  km/s is considerably higher than on the subsequent Sedov phase ( $V_s = (3 - 10) \times 10^3$  km/s), one could expect the production

of CRs with energies  $p > p_{max}$  essentially higher than produced on Sedov phase (Bell and Lucek, 2001). Let us briefly consider this possibility, which was studied by Berezhko and Völk (2004) and by Ptuskin and Zirakashvili (2005).

During the free expansion phase the SN shock evolution is determined by the velocity distribution of the fastest part of the ejecta which is described by a power law

$$dM_{ej}/dv \propto v^{2-k} \quad (13)$$

with  $k = 7$  to  $12$  (Jones et al., 1981; Chevalier, 1982). The ejecta kinetic energy contained in the fraction with speed  $v$  within the interval  $dv$  is  $dE_{ej}(v) \propto v^{4-k}dv$ . The CR spectrum created by the strongly modified shock is quite hard:  $N(p) \propto p^{-\gamma}$ ,  $\gamma < 2$ . For the sake of a rough estimate we assume that all the above ejecta energy goes into CRs with maximum momenta  $p_m(V_s)$ , where the shock speed is roughly the ejecta speed  $V_s \approx v$ . This gives

$$N(p_m)p_m dp_m \propto dE_{ej} \quad (14)$$

in the ultrarelativistic case. Taking into account that  $p_m \propto R_s V_s B \propto V_s^\alpha$ , we obtain

$$\gamma = 2 + (k - 5)/\alpha. \quad (15)$$

Since in the case of uniform ISM  $R_s \propto t^{(k-3)/k}$  we have  $\alpha = (9 - k)/3$  if we suggest for the simplicity  $B_0 \propto \rho_0 V_s^2$ . Even in the case of type Ia SNe with a typical value  $k = 7$  Eq.(15) gives  $\gamma = 5$  (Berezhko and Völk, 2004; Ptuskin and Zirakashvili, 2005). It means that the spectrum of CRs with momenta  $p > p_{max}$  accelerated during the free expansion phase is so steep, that it hardly plays any role for the formation of the GCR spectrum.

In the case of type II/Ib SNe, which are more numerous in our Galaxy (Tammann et al., 1994), during the initial SNR evolutionary phase SN shock propagates through the progenitor star wind. Therefore in this case ambient gas density at the shock front varies as  $\rho_0 \propto R_s^{-2}$  that gives  $\alpha = 2$ . Even at the lowest value  $k = 8$  the resulting CR spectrum is very steep,  $\gamma = 3.5$ .

We therefore conclude, that CRs accelerated during the free expansion phase do not play a role for GCR spectrum, except the case if the actual value of the parameter  $k$  is as small as  $k < 5.4$  for type Ia SNe and  $k < 6$  for type II/Ib SNe or the CSM has more complicated structure than considered above.

In Fig.8 we present GCR energy spectra, expected in the Galaxy, assuming



that SNRs are the main GCR source. Compared with our previous calculations (Berezhko and Ksenofontov, 1999) much higher magnetic field in SNR is used, which varies during the SNR evolution according to Eq.(2). To obtain these spectra  $J(\epsilon_k) \propto J_s(\epsilon_k)\tau_{esc}(R)$  the corresponding source spectra  $J_s(\epsilon_k)$ , produced in SNR during its evolution, were calculated for a typical set of relevant parameters ( $E_{sn} = 10^{51}$  erg,  $M_{ej} = 1.4M_\odot$ ,  $N_H = 0.3 \text{ cm}^{-3}$ ), taking into account their steepening due to the GCR escape from the Galaxy with a time scale  $\tau_{esc} \propto R^{-\mu}$ , where  $R(\epsilon_k)$  is the rigidity,  $\epsilon_k$  is the kinetic energy of CR particle (Berezhko and Völk, 2007).

For a comparison with the experiment we represent in Fig.8 the data of only three experiments, ATIC-2 (Panov et al., 2006), JACEE (Takahashi et al., 1998) and KASCADE (Antoni et al., 2005), which on our view are representative in the corresponding energy ranges. One can see, that the theory in a satisfactory way fits the existing data up to the energy  $\epsilon_k \approx 10^{17}$  eV. The essential exception is the measured in the recent ATIC-2 balloon experiment (Panov et al., 2006) helium spectrum, which opposite to the theoretical expectation is noticeably flatter than the protons spectrum. Note that the spectral shape of protons and helium measured in the previous ATIC-1 experiment at energies  $10 - 10^4$  GeV (Ahn et al., 2006) are very similar. Similar form of the spectra for different GCR nuclei at energies  $\epsilon_k = 10^3 - 10^6$  GeV if observed could be considered as the indirect confirmation of GCR origin in SNRs. Therefore the confirmation of ATIC results for protons and helium by other experiments with comparable or even better precision is very much needed.

Another difficulty for the theory is the fact that to get a consistency with the observed GCR spectra the value  $\mu = 0.75$  is needed, which is a bit beyond the experimentally determined interval  $\mu = 0.3 - 0.7$  (Berezinsky et al., 1990).

In addition, strong energy dependence of the GCR escape time  $\tau_{esc}(\epsilon)$  makes it difficult to interpret the observed CR anisotropy, which is very low, less than one percent at energies  $\epsilon = 10^{15} - 10^{17}$  eV (Hillas, 2005). Here  $\epsilon$  is total energy of CR particle. Total flux of GCRs escaping from the Galaxy  $F_c \propto \epsilon^{-\gamma}$  has energy dependence like CR source spectrum  $J_s \propto \epsilon^{-\gamma}$  with  $\gamma \approx 2$ . Therefore GCR anisotropy outside the region where CR sources are situated (Galactic disk volume) increases with energy  $F_c/J \propto \epsilon^\mu$ , like inverse residence time  $\tau_{esc}^{-1}$ . If  $\mu$  is as big as 0.6 the expected anisotropy at  $\epsilon = 10^{17}$  eV exceeds the level of 100% (Hillas, 2005). Since our observing position is not outside the source layer, we should see a smaller GCR anisotropy (Hillas, 2005). In addition one can also suggest that in the region, occupied by CR sources, GCR diffusion coefficient is higher than in outer part of GCR confinement volume, due to enhanced level of turbulence produced by GCRs streaming away from the Galaxy. In such a case the GCR anisotropy in the source layer could be sufficiently small and consistent with the observations.

Note that the theory predicts concave spectra at energies  $\epsilon > 10Z$  GeV for individual CR species and there are some experimental evidences that the actual GCR spectra are indeed concave, eventhough one needs more precise measurements at  $\epsilon > 10^4$  GeV in order to make more strict conclusion. At the same time calculated all particle spectrum has almost pure power law form up to the knee energy (see Fig.8).

According to Fig.8 the knee in the observed all particles GCR spectrum has to be attributed to the maximum energy of protons, produced in SNRs. The steepening of the all particle GCR spectrum above the knee energy  $3 \times 10^{15}$  eV is a result of progressive depression of contribution of light CR nuclei with the energy increase. Such a scenario is confirmed by KASCADE experiment which shows relatively sharp cutoff spectra of GCR species at energies  $\epsilon_{max} \approx 3Z \times 10^{15}$  eV (Antoni et al., 2005). At energy  $\epsilon \sim 10^{17}$  eV GCR spectrum is dominated by iron nuclei contribution.

According to the analysis, performed by Aloisio et al. (2006) the contribution of Galactic CR sources into the observed GCR spectrum dominates up to the energy  $10^{17}$  eV above which it progressively goes down so that at energy  $10^{18}$  eV the contribution of extragalactic sources becomes dominant. At so-called second knee energy  $\epsilon_k = 5 \times 10^{17}$  eV these two sources provide roughly equal contributions into GCR spectrum. As it is seen from Fig.8, calculations provide a good fit of the observed GCR up to the required energy  $\epsilon_k = 10^{17}$  eV, that is a strong argument for SNRs to be considered as the main Galactic CR source.

Essentially different scenario of the formation of GCR spectrum and the first knee in particular was proposed and discussed by Erlykin and Wolfendale in a series of papers (see Erlykin and Wolfendale, 2000, and references there). Based on the analysis of measurements performed by ground based installations they claim the existence of complex feature of GCR spectrum in the knee energy region. This leads them to a conclusion that observed GCR spectrum consists of smooth background spectrum (without the knee), produced by many CR sources, and superimposed single source (presumably nearby SNR) contribution, that forms a bump on the smooth background spectrum usually interpreted as a (first) knee. The contribution of the single nearby SNR, leading to some peculiarity of GCR spectrum at the detectable level in the knee region, is indeed quite possible (Berezhko and Ksenofontov, 1999). However, the existing measurements of CR composition demonstrate, that the knee is indeed peculiar point in GCR spectrum, where not only the shape of GCR spectrum but also their chemical composition undergoes a noticeable change, that is consistent with CR production in typical SNRs, as described above.

## 5 Summary

Detailed consideration performed within a frame of nonlinear kinetic theory demonstrates that the CR production efficiency in young SNRs is consistent with requirements for the Galactic CR sources. Recent experimental and theoretical studies of Tycho's SNR, RX J1713.7-3946 and SN 1987A provides new very strong evidence for that.

Synchrotron radiation from young SNRs provides evidence that efficient CR acceleration followed by the significant shock modification and magnetic field amplification takes place there. Magnetic field amplification leads to the considerable increase of maximum energy of CRs, accelerated in SNRs. Calculations performed within kinetic nonlinear theory demonstrate that the expected GCR spectrum, produced in SNRs, in satisfactory way fits the existing GCR data up to the energy  $10^{17}$  eV. The first knee in the observed all particles GCR spectrum is attributed to the maximum energy of protons, produced in SNRs. The steepening of the all particle GCR spectrum above the knee energy  $3 \times 10^{15}$  eV is a result of progressive depression of contribution of light CR nuclei with the energy increase. Such a scenario is confirmed by KASCADE experiment which shows relatively sharp cutoff spectra of GCR species at energies  $\epsilon_{max} \approx 3Z \times 10^{15}$  eV (Antoni et al., 2005).

The nature of the whole GCR spectrum, which does not require any significant contribution of galactic CR sources other than SNRs, can be the following. GCR spectrum up to the energy  $\epsilon = 10^{17}$  eV is dominated by the contribution of galactic sources, whereas at  $\epsilon > 10^{18}$  eV GCRs are predominantly extragalactic. Such a picture is consistent with the analysis, presented here, and with the analysis of ultra high energy CR properties (Aloisio et al., 2006) as well. Detail experimental study of GCR spectrum and composition could find whether indeed the transition from galactic to extragalactic component takes place in energy range  $10^{17} - 10^{18}$  eV.

Due to high interior magnetic field in young SNRs the  $\pi^0$ -decay  $\gamma$ -rays generated by the nuclear CR component as a rule dominates over  $\gamma$ -rays, generated by electron CR component, and calculated  $\gamma$ -ray flux fits existing data.

New generation of ground-based  $\gamma$ -ray detectors CANGAROO III, H.E.S.S., MAGIC, VERITAS will presumably measure significantly more accurate  $\gamma$ -ray spectra from already detected SNRs, like Cas A, RXJ1713.7 and Tycho's SNR, as well as from a number of new sources. In this regard considerable interest as a potential  $\gamma$ -ray sources represent Tycho's SNR, SN 1987A and Kepler's SNR (Berezhko et al., 2006) eventhough the expected  $\gamma$ -ray fluxes from these objects only slightly above the sensitivity of modern TeV  $\gamma$ -ray instruments. Together with data, which soon will be obtained by space  $\gamma$ -ray observatory

GLAST, they will reproduce the full  $\gamma$ -ray spectra of some number of individual SNRs, as well as the Galactic background spectrum. Although the existing data together with their theoretical interpretation presents a consistent picture of GCR origin, these new measurements will allow for detailed study of SNRs and the CR production inside them.

## 6 Acknowledgments

This work has been supported by the Russian Foundation For Basic Research (grants 07-02-00221, 06-02-96008, 05-02-16412). The author thanks the organizers of the COSPAR meeting E1.4 "New High-Energy Results on Supernova Remnants and Pulsar Wind Nebula" for the invitation to present this paper and for the financial support, Prof. M.I.Panasyuk and Dr.A.D.Panov for their kind presentation of ATIC-2 data and Prof. H.J.Völk for many useful discussions.

## References

- Acero, A., Ballet, B. Inner density of SN 1006. 36th COSPAR Sci. Assembly, Beijing, Abstracts p.1598, 2006.
- Aharonian, F. A., Akhperjanian, A., Barrio, J., et al. Evidence for TeV gamma ray emission from Cassiopeia A. *Astron. Astrophys.* 370, 112-120, 2001a.
- Aharonian, F.A., Akhperjanian, A.G.,Bazer-Bachi, A.R. et al. High-energy particle acceleration in the shell supernova remnant. *Nature* 432, 75-77, 2004.
- Aharonian, F.A., Akhperjanian, A.G.,Bazer-Bachi, A.R. et al. A detailed spectral and morphological study of the gamma-ray supernova remnant RX J1713.7-3946 with HESS, *Astron. Astrophys.* 449, 223-242, 2006a.
- Aharonian, F.A. , Akhperjanian, A.G.,Bazer-Bachi, A.R. et al. First detection of a VHE gamma-ray spectral maximum from a cosmic source: HESS discovery of the Vela X nebula, *Astron. Astrophys.* 448, L43-L47, 2006b.
- Aharonian, F.A., Akhperjanian, A.G.,Bazer-Bachi, A.R. et al. Primary particle acceleration above 100 TeV in the shell-type supernova remnant RXJ1713.7-3946, *Astron. Astrophys.* 464, 235-243, 2007.
- Ahn, H. S., Seo, E. S., Adams, J. H. et al. The energy spectra of protons and helium measured with the ATIC experiment. *Adv. Space. Res.* 37, 1950-1954, 2006.
- Aloisio, R., Berezhinsky, V., Blasi. P. et al. A dip in the UHECR spectrum and the transition from galactic to extragalactic cosmic rays. arXiv: astro-ph/0608219, 2006.
- Amato, E., Blasi, P. Non-linear particle acceleration at non-relativistic shock

- waves in the presence of self-generated turbulence. *Mon. Not. R. Astron. Soc.* 371, 1251-1258, 2006.
- Antoni, T., Apel, W.D., Badea, A.F. et al. KASCADE measurements of energy spectra for elemental groups of cosmic rays: Results and open problems. *Astropart. Phys.* 24, 1-25, 2005.
- Bell, A.R. The acceleration of cosmic rays in shock fronts.I. *Mon. Not. Roy. Astr. Soc.* 182, 147-156, 1978.
- Bell, A. R., Lucek, S.G. Cosmic ray acceleration to very high energy through the non-linear amplification by cosmic rays of the seed magnetic field. *Mon. Not. Roy. Astr. Soc.* 321, 433-438, 2001.
- Bell, A.R. Turbulent amplification of magnetic field and diffusive shock acceleration of cosmic rays. *Mon. Not. Roy. Astr. Soc.* 353, 550-558, 2004.
- Berezhko, E.G., Krymsky, G.F. Acceleration of cosmic rays by shock waves. *Soviet Phys.-Uspekhi* 31, 27-51, 1988.
- Berezhko, E.G., Yelshin, V.K., Ksenofontov, L.T. Cosmic ray acceleration in supernova remnants. *JETPh* 82, 1-21, 1996.
- Berezhko, E.G. Maximum energy of cosmic rays accelerated by supernova shocks. *Astropart. Phys.*, 5, 367-378, 1996.
- Berezhko, E.G., Völk, H.J. Kinetic theory of cosmic rays and gamma rays in supernova remnants. I. Uniform interstellar medium. *Astropart. Phys.* 7, 183-202, 1997.
- Berezhko, E.G., Ksenofontov, L.T. Composition of cosmic rays accelerated in supernova remnants. *JETPh* 89, 391-403, 1999.
- Berezhko, E.G., Ellison, D.C. A simple model of nonlinear diffusive shock acceleration. *Astrophys. J.* 526, 385-399, 1999.
- Berezhko, E. G., Ksenofontov, L. T. Cosmic Rays, Radio and Gamma-Ray Emission from the Remnant of Supernova 1987A. *Astronomy Letters* 26, 639-656, 2000.
- Berezhko, E.G., Völk, H.J. Kinetic theory of cosmic ray and gamma-ray production in supernova remnants expanding into wind bubbles. *Astron. Astrophys.* 357, 283-300, 2000a.
- Berezhko, E.G., Völk, H.J. Theory of synchrotron emission from supernova remnants. *Astron. Astrophys.* 427, 525-536, 2004.
- Berezhko, E.G. Gamma-ray astronomy and cosmic ray origin problem. *Adv. Space Res.*, 35, 1031-1040, 2005
- Berezhko, E.G., Völk, H.J. Theory of cosmic ray production in the supernova remnant RX J1713.7-3946. *Astron. Astrophys.* 451, 981-990, 2006.
- Berezhko, E.G., Ksenofontov, L. T., Völk, H.J. Gamma-ray emission expected from Kepler's supernova remnant. *Astron. Astrophys.* 452, 217-221, 2006.
- Berezhko, E. G., Ksenofontov, L. T. Magnetic field in supernova remnant SN 1987A. *Astrophys. J.* 650, L59-L62, 2006.
- Berezhko, E. G., Völk, H. J. Spectrum of cosmic rays, produced in supernova remnants. *Astrophys. J.* 661, L175-178, 2007.
- Berezinsky, V.S., Bulanov, S.V., Ginzburg, V.L., et al. 1990, *Astrophysics of Cosmic Rays*, North-Holland Publ. Comp.

- Blandford, R., Eichler, D. Particle acceleration in astrophysical shocks: a theory of cosmic ray origin. *Phys. Rep.* 154, 1-75, 1987.
- Cassam-Chenaï, G., Decourchelle, A., Ballet, J., et al. XMM-Newton observations of the supernova remnant RX J1713.7-3946 and its central source observations of SNR RX J1713.7-3946. *Astron. Astrophys.* 427, 199-216, 2004.
- Chevalier, R.A. Self-similar solutions for the interaction of stellar ejecta with an external medium. *Astrophys.J.* 258, 790-797, 1982.
- Chevalier, R. A., Fransson, C. Circumstellar matter and the nature of the SN1987A progenitor star. *Nature*, 328, 44-45, 1987.
- Chevalier, R.A., Blondin, J.M., Emmering, R.T. Hydrodynamic instabilities in supernova remnants - Self-similar driven waves. *Astrophys. J.* 392, 118-130, 1992.
- Chevalier, R. A., Dwarkadas, V. V. The Presupernova H II Region around SN 1987A. *Astrophys. J.* 452, L45-L48, 1995.
- Decourchelle, A., Ellison, D.C., Ballet, J. Thermal X-ray Emission and Cosmic Ray Production in Young Supernova Remnants. *Astrophys. J.* 543, L57-L60, 2000.
- Drury, L. O'C., Völk, H. J., Berezhko, E. G. Existence and interpretation of smooth cosmic-ray dominated shock structures in supernova remnants. *Astron. Astrophys.* 299, 222-224, 1995.
- Drury, L'O.C. An introduction to the theory of diffusive shock acceleration of energetic particles in tenuous plasmas. *Rep. Progr. Phys.* 46, 973-1027, 1983.
- Enomoto, R., Tanimori, T., Naito, T., et al. The acceleration of cosmic-ray protons in the supernova remnant RX J1713.7-3946 *Nature* 416, 823-826, 2002.
- Erlykin, A.D., Wolfendale, A.W. The origin of PeV cosmic rays. *Astron. Astrophys.* 356, L63-L65, 2000.
- Gaensler, B. M., Manchester, R. N., Staveley-Smith, L. et al. The Asymmetric Radio Remnant of SN 1987A. *Astrophys. J.* 479, 845-860, 1997
- Gorenstein, P., Hughes, J. P., Tucker, W. H. *Astrophys. J.* 420, L25-L28, 1994.
- Hasinger, G., Ashenbach, B., Trümper, J. The X-ray lightcurve of SN 1987A. *Astron. Astrophys.* 312, L9-L12, 1996.
- Hillas, A. M. Can diffusive shock acceleration in supernova remnant account for high-energy galactic cosmic rays?. *J. Phys. G: Nucl. Part. Phys.* 31, R95-R131, 2005.
- Hiraga, J.S., Uchiyama, Y., Takahashi, T., Aharonian, F.A. Spectral properties of nonthermal X-ray emission from the shell-type SNR RX J1713.7 3946 as revealed by XMM-Newton *Astron. Astrophys.* 431, 953-961, 2005.
- Jones, E.M., Smith, B.W. & Straka, W.C. Formation of supernova remnants - The pre-blast-wave phase. *Astrophys. J.* 249, 185-194, 1981.
- Jones, F.C., Ellison, D.C. The plasma physics of shock acceleration. *Space Sci. Rev.* 58, 259-346, 1991.
- Koyama, K., Kinagasa K., Matsuzaki, K., et al. Discovery of Non-Thermal

- X-Rays from the Northwest Shell of the New SNR RX J1713.7-3946: The Second SN 1006? PASJ 49, L7-L11, 1997.
- Ksenofontov, L. T., Berezhko, E. G. and Völk, H. J. Dependence of the gamma-ray emission from SN 1006 on the astronomical parameters. *Astron. Astrophys.* 443, 973-980, 2005.
- Lagage, P. O., Cesarsky, C. J. The maximum energy of cosmic rays accelerated by supernova shocks. *Astron. Astrophys.* 125, 249-257, 1983.
- Lazendic, J. S., Slane, P.O., Gaensler, B.M., et al. A High-Resolution Study of Nonthermal Radio and X-Ray Emission from Supernova Remnant G347.3-0.5. *Astrophys. J.* 602, 271-285, 2004.
- Lucek, S.G., Bell, A.R. Non-linear amplification of a magnetic field driven by cosmic ray streaming. *Mon. Not. Roy. Astr. Soc.* 314, 65-74, 2000.
- Malkov, M.A., Drury, L.O'C. Nonlinear theory of diffusive acceleration of particles by shock waves. *Rep. Progr. Phys.* 64, 429-481, 2001.
- Malkov, M. A., Diamond, P.H., Sagdeev, R.Z. On the Gamma-Ray Spectra Radiated by Protons Accelerated in Supernova Remnant Shocks near Molecular Clouds: The case of Supernova Remnant RX J1713.7-3946. *Astrophys. J.* 624, L37-L40, 2005.
- Manchester, R. N., Gaensler, B. M., Wheaton, V. C., et al. Evolution of the Radio Remnant of SN 1987A: 1990-2001. *PASA* 19, 207-221, 2002.
- Manchester, R. N., Gaensler, B. M. Supernova 1987A in the Large Magellanic Cloud. *IAU Circ.* 7757, 2001.
- McCray, R. Supernova 1987A revisited. *Annual Rev. Astron. Astrophys.* 31, 175-216, 1993.
- McKenzie, J.F., Völk, J.H. Non-linear theory of cosmic ray shocks including selfgenerated Alfvén waves. *Astron. Astrophys.* 116, 191-200, 1982.
- Michael, E., Zhekov, S., McCray, R., et al. The X-Ray Spectrum of Supernova Remnant 1987A *Astrophys. J.* 574, 166-178, 2002.
- Muraishi, H., Tanimori, T., Yanagita, S. et al. Evidence for TeV gamma-ray emission from the shell type SNR RX J1713.7-3946. *Astron. Astrophys.* 354, L57-L61, 2000.
- Panov, A. D., Adams, J. H., Ahn, H. S. et al. The results of ATIC-2 experiment for elemental spectra of cosmic rays, <arXiv:astro-ph/0612377>2006.
- Parizot, E., Marcowith, A., Ballet, J., Gallant, Y. A. Observational constraints on energetic particle diffusion in young supernovae remnants: amplified magnetic field and maximum energy. *Astron. Astrophys.* 453, 387-395, 2006.
- Park, S. Zhekov, S. A., Burrows, D. N. et al. A Chandra View of the Morphological and Spectral Evolution of Supernova Remnant 1987A *Astrophys. J.* 610, 275-284, 2004.
- Pelletier, G., Lemoine, M., Marcowith, A. Turbulence and particle acceleration in collisionless supernovae remnant shocks. I-Anisotropic spectra solutions. *Astron. Astrophys.* 453, 181-191, 2006.
- Pfeffermann, E., Aschenbach, B. 1996, in *Roentgenstrahlung from the Universe*, ed. H.H. Zimmermann, J. Trümper, & H. Yorke (MPE Rep. 263; Garching: MPE), 267.

- Ptuskin, V.S., Zirakashvili, V.N. On the spectrum of high-energy cosmic rays produced by supernova remnants in the presence of strong cosmic-ray streaming instability and wave dissipation. *Astron. Astrophys.* 429, 755-765, 2005.
- Reynolds, S.P., Ellison, D.C. Electron acceleration in Tycho's and Kepler's supernova remnants - Spectral evidence of Fermi shock acceleration. *Astrophys. J.* 399, L75-L78, 1992.
- Reynolds, P.T., Akerlof, C.W., Cawley, M.F. et al. Survey of candidate gamma-ray sources at TeV energies using a high-resolution Cerenkov imaging system - 1988-1991. *Astrophys. J.* 404, 206-218, 1993.
- Slane, P., Gaensler, B.M., Dame, T.M., et al. Nonthermal X-Ray Emission from the Shell-Type Supernova Remnant G347.3-0.5. *Astrophys. J.* 525, 357-367, 1999.
- Staveley-Smith, L. Manchester, R. N., Kesteven, M. J. et al. Birth of a radio supernova remnant in supernova 1987A. *Nature* 355, 147-149, 1992.
- Tammann, G.A., Löffler, W., Schröder, A. The Galactic supernova rate. *Astrophys. J. Suppl.* 92, 487-493, 1994.
- Tan, S.M., Gull, S.F. The expansion of Tycho's supernova remnant as determined by a new algorithm for comparing data. *Mon. Not. Roy. Astr. Soc.* 216, 949-970, 1985.
- Takahashi, Y., Asakimori, K., Burnett, T.H. et al. Elemental Abundance of High Energy Cosmic Rays *Nuclear Phys. B (Proc. Suppl.)* 60, 83-92, 1998.
- Turtle, A. J., Campbell-Wilson, D., Bunton, J. D. et al. A prompt radio burst from supernova 1987A in the Large Magellanic Cloud. *Nature* 327, 38-40, 1987.
- Vladimirov, A., Ellison, D. C., Bykov, A. Nonlinear Diffusive Shock Acceleration with Magnetic field Amplification. *Astrophys. J.* 652, 1246-1258, 2006.
- Völk, H.J., Berezhko, E.G., Ksenofontov, L.T., Rowell, G.P. The high energy gamma-ray emission expected from Tycho's supernova remnant. *Astron. Astrophys.* 396, 649-656, 2002.
- Völk, H.J., Berezhko, E.G., Ksenofontov, L.T. Variation of cosmic ray injection across supernova shocks. *Astron. Astrophys.* 409, 563-571, 2003.
- Völk, H.J., Berezhko, E.G., Ksenofontov, L.T. Magnetic field amplification in Tycho and other shell type supernova remnants. *Astron. Astrophys.* 433, 229-240, 2005.
- Völk, H.J., Berezhko, E.G., Ksenofontov, L.T. New evidence for strong non-thermal effects in Tycho's SNR. Accepted in *Astrophys. Space Sci.* 2006.
- Uchiyama, Y., Aharonian, F.A. & Takahashi, T. Fine-structure in the nonthermal X-ray emission of SNR RX J1713.7-3946 revealed by Chandra. *Astron. Astrophys.* 400, 567-574, 2003.
- Wang, C.-Y., Chevalier, R.A. Instabilities and Clumping in Type IA Supernova Remnants. *Astrophys. J.* 549, 1119-1134, 2001.
- Warren, J.S., Hughes, J.P. Badenes, C. et al. Cosmic-Ray Acceleration at the Forward Shock in Tycho's Supernova Remnant: Evidence from Chandra X-Ray Observations. *Astrophys. J.* 634, 376-389, 2005.



Winkler, P. F., Gupta, G. and Long, K. S. The SN 1006 Remnant: Optical Proper Motions, Deep Imaging, Distance, and Brightness at Maximum. *Astrophys. J.* 585, 324-335, 2003.

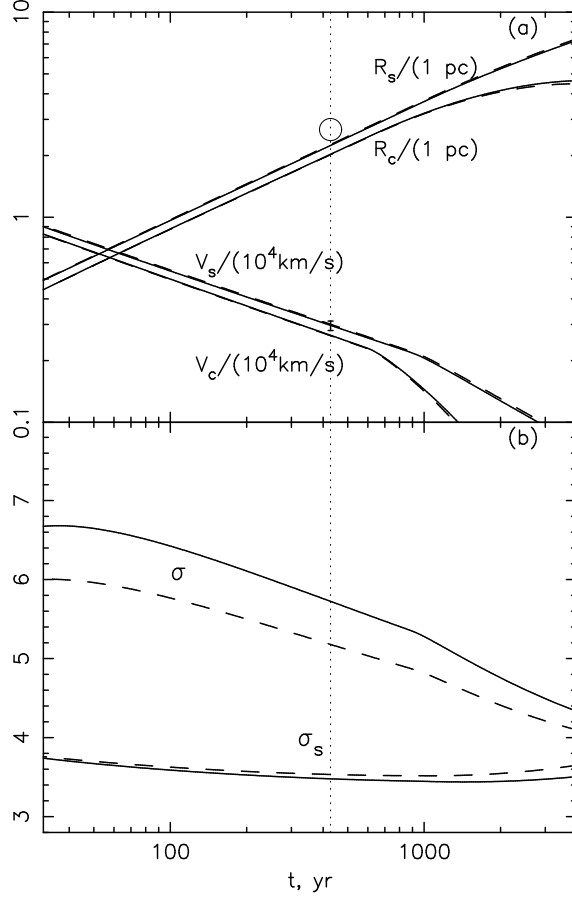


Fig. 1. (a) Shock radius  $R_s$ , contact discontinuity radius  $R_c$ , shock speed  $V_s$ , and contact discontinuity speed  $V_c$ , for Tycho's SNR as functions of time, including particle acceleration; (b) total shock ( $\sigma$ ) and subshock ( $\sigma_s$ ) compression ratios (Völk et al., 2006). The *dotted vertical line* marks the current epoch. The *solid and dashed lines* correspond to the internal magnetic field strength  $B_d = 240 \mu\text{G}$  and ( $B_d = 360 \mu\text{G}$ ), respectively. The observed mean size and speed of the shock, as determined by radio measurements (Tan and Gull, 1985), are shown as well.

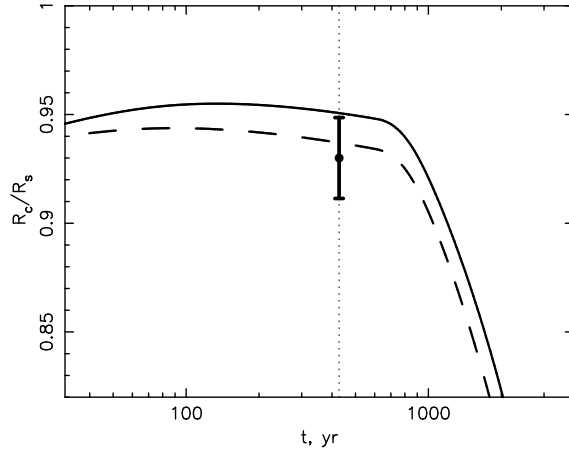


Fig. 2. The ratio  $R_c/R_s$  of the radii of the contact discontinuity and the forward shock of Tycho's SNR as a function of time (Völk et al., 2006). Solid and dashed lines correspond to the same two cases as in Fig.1. The experimental point is taken from Warren et al. (2005).

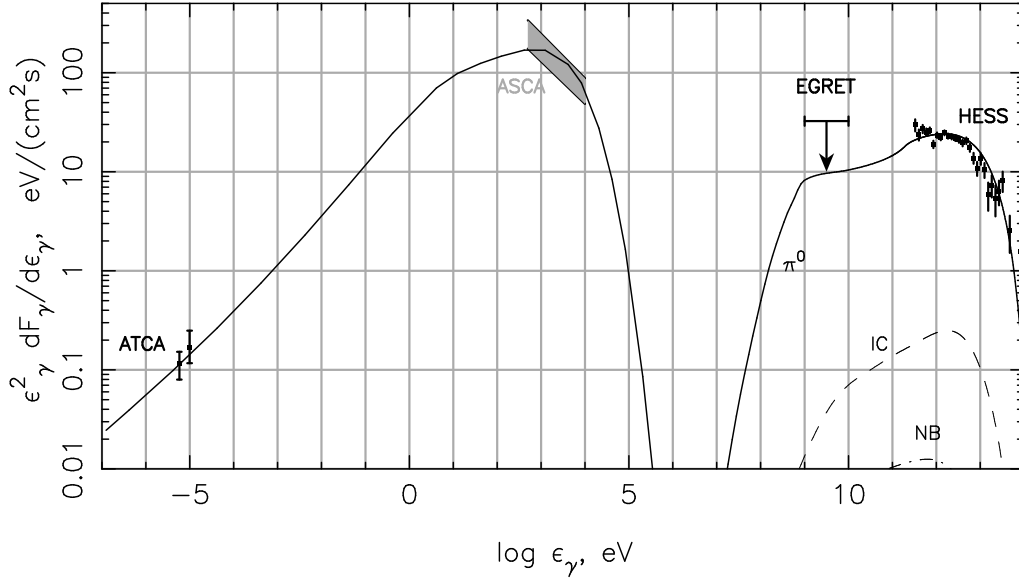


Fig. 3. Spatially integrated spectral energy distribution of RX J1713.7-3946 (Berezhko and Völk, 2006). The ATCA radio data (cf. Aharonian et al., 2006a), ASCA X-ray data (cf. Aharonian et al., 2005), and H.E.S.S. data (Aharonian et al., 2007) are shown. The EGRET upper limit for the RX J1713.7-3946 position (Aharonian et al., 2005) is shown as well. The solid curve at energies above  $10^7$  eV corresponds to  $\pi^0$ -decay  $\gamma$ -ray emission, whereas the dashed and dash-dotted curves indicate the inverse Compton (IC) and Nonthermal Bremsstrahlung (NB) emissions, respectively.

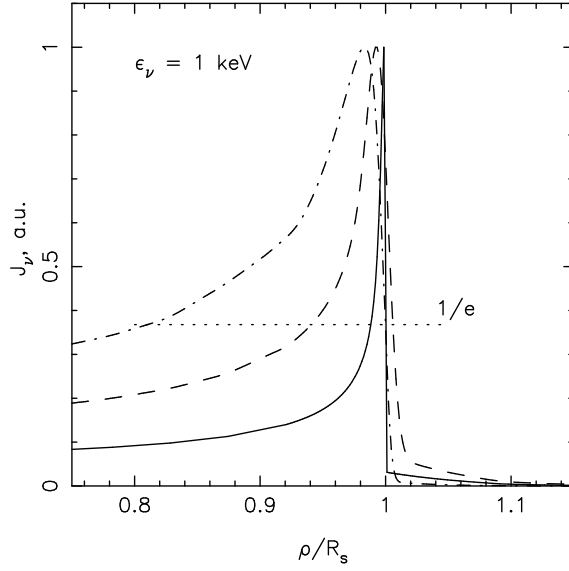


Fig. 4. Projected radial profile of the X-ray synchrotron emission for the energy  $\epsilon_\nu = 1$  keV from RX J1713.7-3946 (Berezhko and Völk, 2006). The solid line corresponds to the high-injection model; the dashed line again represents the above profile, but smoothed to the resolution of the XMM-Newton data used in Hiraga et al. (2005); the dash-dotted line corresponds to the test-particle limit.

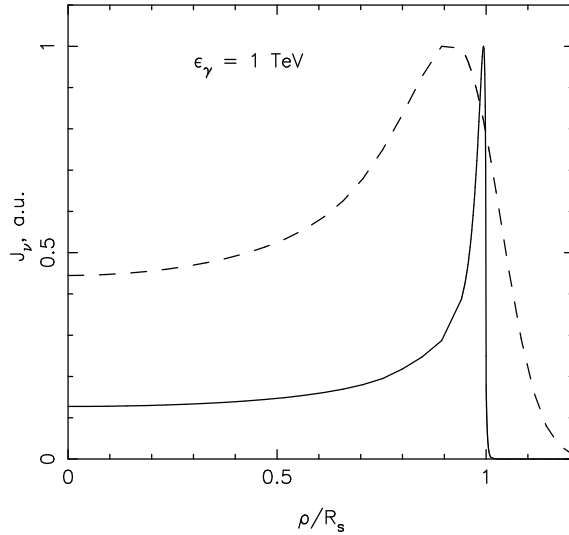


Fig. 5. The projected radial profile of  $\gamma$ -ray emission for  $\gamma$ -ray energies  $\epsilon_\gamma = 1$  TeV (Berezhko and Völk, 2006). The calculated radial profile is given by the solid line; the dashed line represents the calculated profile smoothed with a Gaussian point spread function of the width  $\sigma_\psi = 0.05^\circ$ . For purposes of presentation both profiles are normalised to their peak values in this figure.

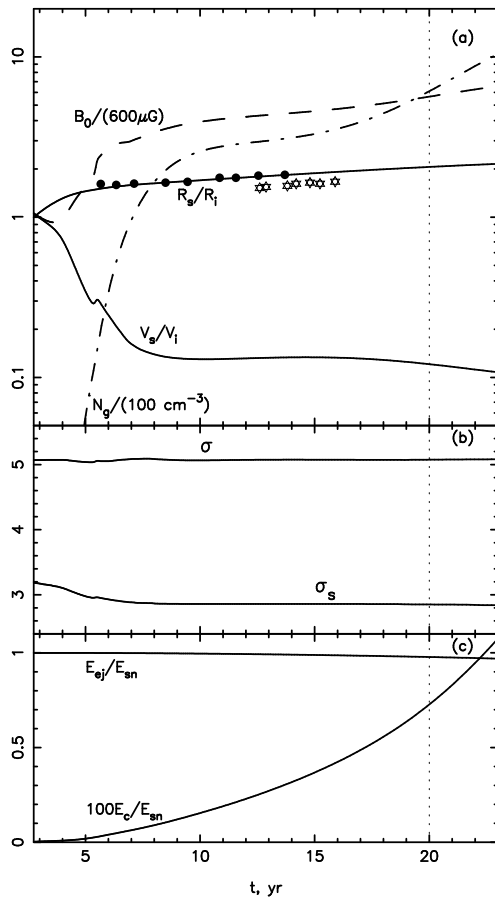


Fig. 6. (a) Shock radius  $R_s$ , shock speed  $V_s$ , gas density  $N_g$  and upstream magnetic field  $B_0$  at the current shock position; (b) total shock ( $\sigma$ ) and subshock ( $\sigma_s$ ) compression ratios; (c) kinetic energy of ejecta  $E_{ej}$  and accelerated CR energy content  $E_c$  as functions of time for SN 1987A (Berezhko and Ksenofontov, 2006). The observed radius of the SN shock, as determined by radio (Manchester et al., 2002) and X-ray measurements (Park et al., 2004), are shown by circles and stars respectively. The scaling values are  $R_i = R_T = 3.1 \times 10^{17}$  cm and  $V_i = 28000$  km/s. The *dotted vertical line* marks the current epoch.

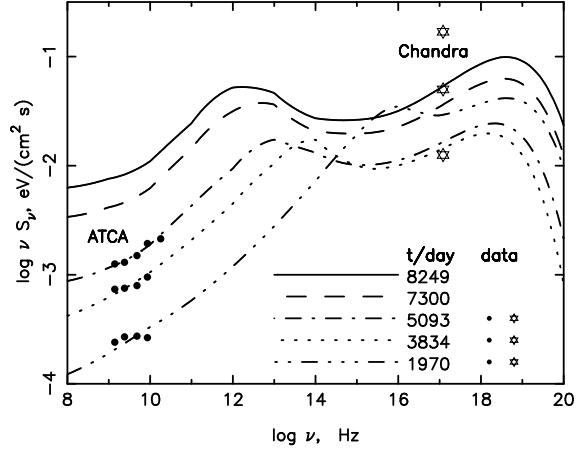


Fig. 7. Synchrotron energy spectrum of SN 1987A, calculated for the five evolutionary epochs Berezhko and Ksenofontov (2006). The ATCA radio (Manchester et al., 2002; Manchester and Gaensler, 2001) and Chandra X-ray (Park et al., 2004) data for three epochs are shown as well. Higher measured fluxes correspond to later epoch.

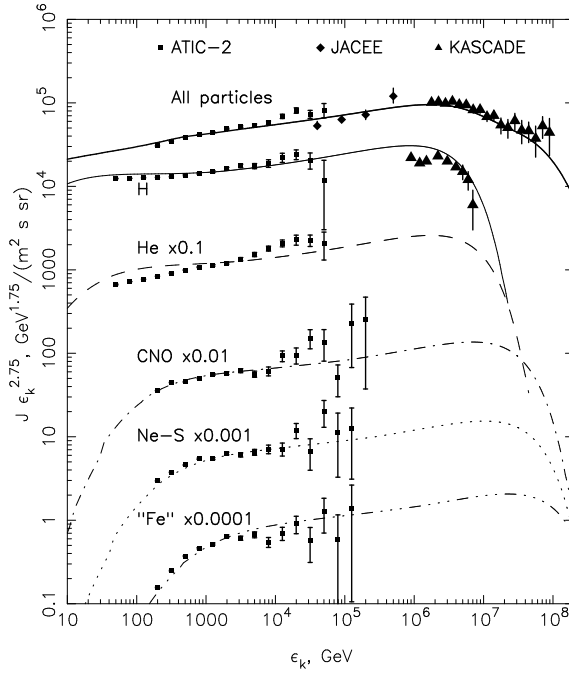


Fig. 8. Energy spectra for five groups of abundant GCR nuclei and all particles spectrum (Berezhko and Völk, 2007). The data of ATIC-2 (Panov et al., 2006), JACEE (Takahashi et al., 1998) and KASCADE (Antoni et al., 2005) experiments are shown as well.